RSC Advances

PAPER

View Article Online
View Journal | View Issue

Cite this: *RSC Adv.*, 2020, **10**, 10758

Fabrication of mechanically resistant superhydrophobic synthetic suede materials

Xiang-Dong Luo,[ac] Chao-Hua Xue, *[ab] Ren-Xuan Wei,[a] Wei-Hao Wang,[a] Mi-Mi Du,[a] Meng-Chen Huang[a] and Hui-Gui Li[a]

Received 19th December 2019
Accepted 9th March 2020

DOI: 10.1039/c9ra10708h

rsc.li/rsc-advances

Functionalization of synthetic suede materials with excellent superhydrophobicity can expand their application ranges. Superhydrophobic synthetic suede was obtained by coating with polydimethylsiloxane (PDMS) and octadecyltrichlorosilane (OTS). Utilizing the synthetic suede effect of the fibrous rough structures in combination with the low surface energy micro–nano rough structure on fibers resulting from PDMS and OTS, the surface was easily turned superhydrophobic with self-cleaning properties. Abrasion tests showed that the superhydrophobic synthetic suede has excellent superhydrophobic performance after more than 2000 severe abrasion tests. This research provides a facile strategy for the preparation of practical superhydrophobic synthetic suede materials.

Introduction

High water repellency can be observed in nature, for example, on lotus leaves, rose petals and animal feathers.[1–5] Those materials are referred to as superhydrophobic surfaces with a water contact angle (CA) greater than 150° and water sliding angle (SA) typically lower than 10°.[6–10] They can be used in potential applications including oil–water separation,[18–20] self-cleaning,[21–23] anti-corrosion,[24–26] anti-fog[27] and others[28–30] due to their water-repellency[11–14] and self-cleaning properties.[15–17] Up to now, quite an army of superhydrophobic surfaces have been prepared on various substrates such as glass, metal, wood, sponges, and textiles.[31–34] However, little attention has been paid to the construction of superhydrophobic synthetic suede which is a classical flexible substrate widely used in the wearable field.[35–38] Synthetic suede is a kind of synthetic leather material with hydrophilicity because of the superfine nylon fibers in the substrate, which have an abundance of hydrophilic groups,[39,40] such as –OH, –CO–, and –NH– of the macromolecules in nylon, which can form hydrogen bonds with water molecules. Since there is a sea of fine fluff on the surface, the synthetic suede products are vulnerable to liquid stain or easily contaminated by blotting. Making the synthetic suede superhydrophobic and giving it self-cleaning properties could be a good way to solve these problems. Additionally, turning daily materials superhydrophobic can make life much more convenient, and prolong the life span of the materials. Since the surface of such substrates inevitably experiences all kinds of friction in practical applications, so much attention has been paid to promote the wear resistance of superhydrophobic flexible materials in recent years.[41–49] One approach to create a durability of superhydrophobic surfaces is to endow materials with the ability to regenerate the surface roughness or restore the hydrophobic components. Zhang *et al.*[50] reported a long lasting superhydrophobic surfaces by spraying polystyrene/SiO_2 core/shell particles as a coating skeleton and polydimethylsiloxane (PDMS) as hydrophobic interconnection. The coating exposed new roughening structures during the rubbing process, thus maintaining a suitable hierarchical roughness, favouring the superhydrophobic property of the surface. Also, the superhydrophobicity of the damaged surface could be automatically restored in 12 h at room temperature. Another approach to increase the life time of superhydrophobic materials is to use mechanically durable hydrophobic materials. Zhao *et al.*[51] coated three kinds of nano-silica with different particle sizes by PDMS and sprayed them on the glass substrate to prepare superhydrophobic surfaces with a water contact angle of 169.8° and rolling angle of less than 4°. The persistent superhydrophobic properties were maintained within 6 months. In addition, the coating also has good mechanical stability and remarkable self-cleaning property. Wang *et al.*[52] prepared transparent superhydrophobic coating by a simple method, in which PDMS was used as the intermediate layer to coat the glass, and silica nanoparticles with fluoroalkyl silanes were embedded on the surface of PDMS. The obtained coating maintained superhydrophobicity and self-cleaning property.

Inspired by these works, and based on utilizing the characteristics of the fine roughening structures of suede,[53,54] here we report a facile method to fabricate wear resistant superhydrophobic synthetic suede. As shown in Fig. 1, pristine

[a]*College of Bioresources Chemical and Materials Engineering, Shaanxi University of Science and Technology, Xi'an 710021, China. E-mail: xuechaohua@126.com*
[b]*National Demonstration Center for Experimental Light Chemistry Engineering Education, Shaanxi University of Science and Technology, Xi'an 710021, China*
[c]*College of Design and Art, Shaanxi University of Science and Technology, Xi'an 710021, China*

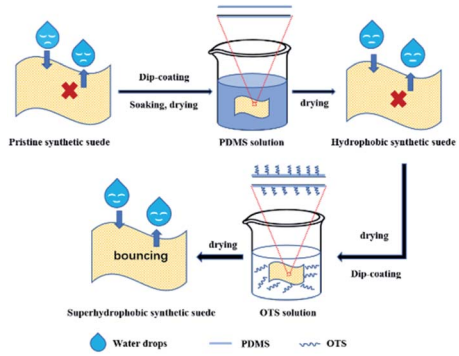

Fig. 1 Schematic illustration of the fabrication of superhydrophobic synthetic suede.

synthetic suede was soaked in PDMS then in OTS solution to obtain superhydrophobic synthetic suede after drying. Abrasion tests showed that the superhydrophobic synthetic suede was robust to machine wearing, maintaining its superhydrophobicity even after 2000 abrasion cycles.

Experimental

Materials

Synthetic suede was purchased from Anhui Anli synthetic Leather Co., Ltd, which was rinsed with ethanol and distilled water before use. Polydimethylsiloxane (PDMS, Sylgard 184 Silicone Elastomer Kit with components of PDMS base and curing agent) was purchased from DOW CORNING. Octadecyltrichlorosilane (OTS was purchased from Shanghai Macklin Biochemical Co., Ltd). Ethanol and *n*-hexane were obtained from Tianjin Fuyu Fine Chemical Company. All other chemicals were used as received without further purification.

Fabrication of superhydrophobic synthetic suede

Several synthetic suede samples (3 cm × 2.5 cm) were washed with anhydrous ethanol and distilled water to remove dust and dirt on the surface, and then dried for 10 min (60 °C). A PDMS solution was prepared by dissolving 0.2 g of PDMS base and 0.02 g of curing agent into 20 g of *n*-hexane solution, followed by ultrasonication for 15 min. An OTS solution was prepared by dissolving different mass fractions (OTS to *n*-hexane ratio) of OTS into 20 g of *n*-hexane solution under stirring. Typically, synthetic suede samples were immersed in the PDMS solution for 40 min and taken out to dry at 70 °C for 10 min to obtain Synthetic suede–PDMS. Then the Synthetic suede–PDMS samples were immersed in the OTS solution for 30 min and taken out to dry at 70 °C for 10 min to obtain Synthetic suede–PDMS–OTS.

Characterization

Scanning electron microscopy (SEM) images were obtained using a Hitachi S-4800 field emission scanning electron microscope operated at an acceleration voltage of 5 kV. All samples were sputter-coated with gold prior to examination. Water contact angles of the synthetic suede were measured using a video optical contact angle system (OCA 20, Data physics, Germany) with deionized water droplet of 5 μL at room temperature. By adjusting the tilt angle of the sample to make water drops (10 μL) roll off the synthetic suede surface, sliding angle (SA) was obtained. The reported values of CA and SA were determined by averaging values measured at five different points on each sample surface. All samples were analysed by Fourier transform infrared spectroscopy (FTIR, Bruker TENSOR27, Germany).

Stability evaluation of superhydrophobic synthetic suede

Abrasion resistance was tested according to a modified procedure based on the AATCC Test Method 8-2001, according to our previous work.[55] The as-coated synthetic suede was abraded by a nylon textile fixed onto the stainless-steel column and moved repeatedly with a load pressure of 45 kPa and a moving path of 100 mm. In the test, two moving paths form one cycle. After certain cycles of abrasion, the CAs on the rubbed area of the samples were tested.

Chemical stability

Aqueous solutions with different pH were used to test the chemical stability of superhydrophobic synthetic suede. The samples were immersed into the selected solutions for 72 h, and thoroughly rinsed with deionized water and dried at 80 °C for CA test.

Results and discussion

Morphology and composition of synthetic suede

SEM images of the pristine synthetic suede, Synthetic suede–PDMS, Synthetic suede–OTS and Synthetic suede–PDMS–OTS were shown in Fig. 2(a–d). It was found that the fiber surfaces of the pristine synthetic suede are quite smooth with a diameter of about 2.86 μm (Fig. 2(a)). Coating of PDMS did not cause obvious change in the morphology of the fiber surface of the synthetic suede while the diameter of the fiber increased to

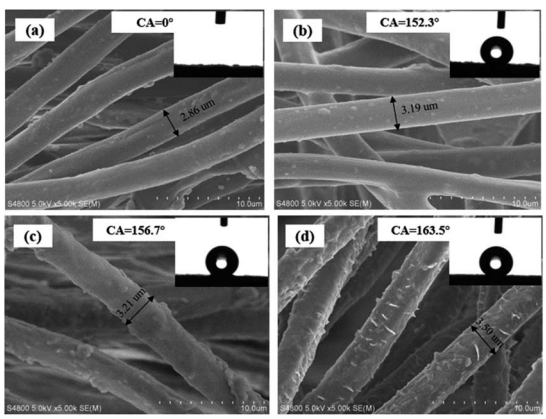

Fig. 2 SEM images of (a) pristine synthetic suede, (b) Synthetic suede–PDMS and (c) Synthetic suede–OTS, (d) Synthetic suede–PDMS–OTS.

about 3.19 μm, which becomes thicker, as shown in Fig. 2(b). When the sample was only treated with OTS, the surfaces of fibers became rougher than ever with some bulges (Fig. 2(c)). When the samples were treated with PDMS followed by OTS, the surface of the fiber became covered by much more micro–nano bulges and spiny structure, the fiber increased to about 3.50 μm as shown in Fig. 2(d), which may be caused by the self-dehydrating and condensation of OTS on the Synthetic suede–PDMS. It should be noticed that when PDMS or OTS was used alone to modify the synthetic suede, the value of CA can reach more than 150°, the value of SA can reach more than 8°. This is because OTS and PDMS can dramatically reduce the low surface energy of the suede surface, making the microscale roughening suede with fluffy microstructure superhydrophobic. However, due to insufficient surface roughness in nanoscale, the rolling angle is relatively large, and water droplets are not easy to roll down from the surface, thus affecting the self-cleaning effect of the surface. When the samples were treated with PDMS and OTS together, the value of CA can reach 163.5° and the value of SA can reach less than 5° due to decoration of these low surface energy nanoscale spiny structures on the fiber surfaces, which not only hydrophobized the surface but also provided a higher roughening structure, enhancing the superhydrophobicity on the synthetic suede.

The element distribution of the Synthetic suede–PDMS and Synthetic suede–PDMS–OTS were illustrated by EDS, as shown in Fig. 3(a–d). The dominant elements (C, O and Si) were uniformly distributed on the Synthetic suede–PDMS and Synthetic suede–PDMS–OTS, demonstrating PDMS was eventually coated on the synthetic suede surface. There was no Cl in Synthetic suede–PDMS, while the content of Cl in Synthetic suede–PDMS–OTS was 4.20% (Fig. 3(d)). This might be caused by the OTS accumulation[56] on the surface of PDMS coating through self-dehydrated condensation, forming OTS condensed polyoctadecylsiloxane attached to PDMS by van der Waals forces. Due to the incomplete reaction of the self-dehydration condensation and possible residuals of chlorine from OTS, the content of the chlorine element appeared in the sample of Synthetic suede–PDMS–OTS, implying the successful coating of OTS on the synthetic suede.

As shown in Fig. 4, FTIR spectra showed the changes of the functional groups of the synthetic suede. The peak at 3304 and 1543 cm^{-1} and a strong absorption band at around 1642 cm^{-1} was related to the $-NH_2$ and CONH groups, which are characteristic peaks of the pristine synthetic suede[57] with 2920 cm^{-1} and 2853 cm^{-1} related to the –CH antisymmetric and symmetric stretching. After PDMS coating, a broad band centred at 1080 cm^{-1} and 804 cm^{-1} appeared, which were associated with the Si–O–Si and Si–CH_3 asymmetric bond stretching vibration peaks derived from PDMS.[58] By comparing Synthetic suede–PDMS–OTS with Synthetic suede–PDMS, it can be found that the peak appears at 1465 cm^{-1} related to $-CH_2$ bending (scissors) vibration. These results further confirmed the coating of PDMS followed by condensed OTS on the fibers.

The dosage of OTS played a crucial role in determining the surface morphology and wetting behaviour. From the SEM images in Fig. 5(a–e), it was found that, with increasing the OTS concentration, the fiber surface became roughened and nanoscale thorn structures appeared when the OTS concentration reached 1.5% as show in Fig. 5(c). The nanoscale thorn structures on the fiber surface in combination with the microscale woven structures as well as the fluffy characteristics of the suede made the suede have typical micro/nano structures, enhancing the superhydrophobicity of the suede material. However, Fig. 5(d and e) show that further increase of OTS concentration did not contribute much to the roughening of the fiber surface as well as the CA value (Fig. 5(f)).

Surface wettability

As shown in Fig. 6(a), the pristine synthetic suede was easily wetted by water drops with different colour due to the capillary effect and the abundant hydrophilic hydroxyl groups of the synthetic suede. However, the water droplets were spherical on the sample of Synthetic suede–PDMS–OTS, exhibiting remarkable superhydrophobicity. In addition, contact angle measurement showed the value of CA is 162.8° and SA is 3.4° on the as-prepared superhydrophobic synthetic suede. To further

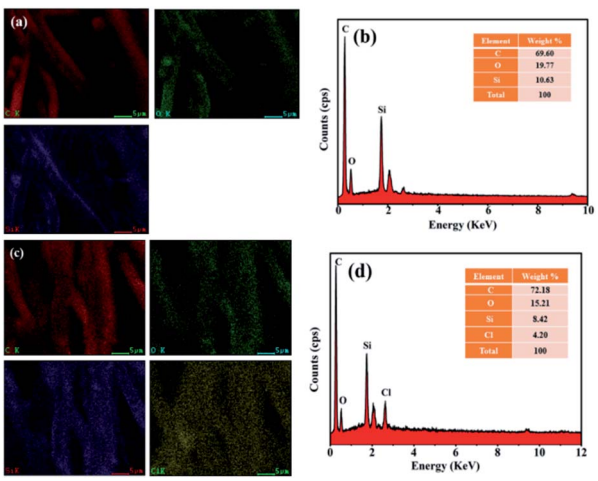

Fig. 3 Element mapping (a) and EDS spectrum (b) of Synthetic suede–PDMS; element mapping (c) and EDS spectrum (d) of Synthetic suede–PDMS–OTS.

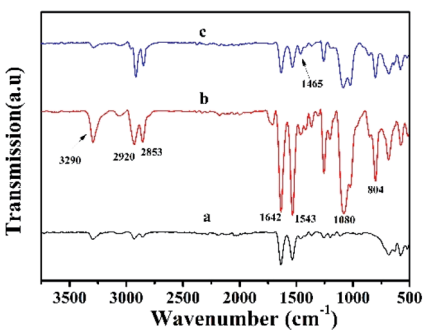

Fig. 4 FTIR spectra of (a) pristine synthetic suede, (b) Synthetic suede–PDMS, and (c) Synthetic suede–PDMS–OTS.

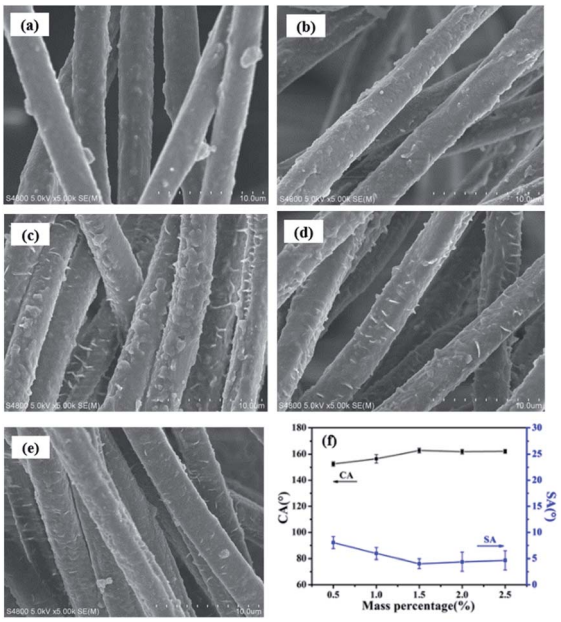

Fig. 5 SEM images of the Synthetic suede–PDMS–OTS with different mass fractions of OTS. (a) 0.5%, (b) 1.0%, (c) 1.5%, (d) 2.0% (e) 2.5%; (f) CA changes of Synthetic suede–PDMS–OTS with different mass fractions of OTS.

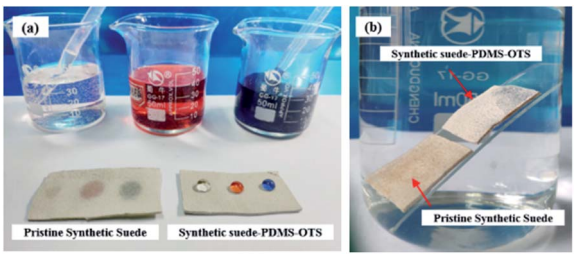

Fig. 6 The pictures of (a) water drops on pristine synthetic suede and Synthetic suede–PDMS–OTS and (b) immersion of pristine synthetic suede and Synthetic suede–PDMS–OTS stuck on glass.

demonstrate the water-repellent property of the superhydrophobic synthetic suede, the pristine synthetic suede and Synthetic suede–PDMS–OTS samples were stuck on a glass plate and immersed into water. It was found mirror-like phenomenon was displayed obviously on the surface of the Synthetic suede–PDMS–OTS, as shown in Fig. 6(b). This is because the low surface energy material loaded on the synthetic suede in combination with its rough structure made the material superhydrophobic and easy to trap air at the interface to prevent the material from being soaked with water.

Durability of the superhydrophobic synthetic suede

The wear of the synthetic suede usually comes from the contact friction and washing friction with each other, which belong to physical damage and will affect the hydrophobic effect of the surface. Therefore, we tested the wear resistance of the synthetic suede with a friction meter. As shown in Fig. 7(a), the droplets

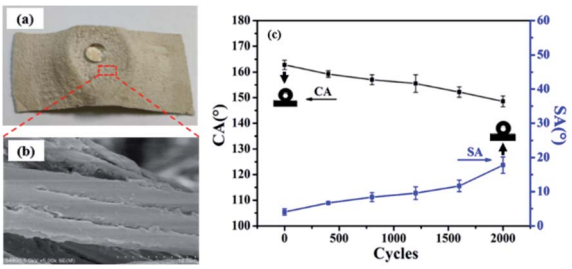

Fig. 7 Pictures of the Synthetic suede–PDMS–OTS after 2000 abrasions (a) and SEM images of (b); (c) CA and SA changes of Synthetic suede–PDMS–OTS with abrasion cycles.

can still maintain the spherical shape on the synthetic suede after 2000 cycle abrasion. Fig. 7(c) showed that the CA slightly decreased with the increase of wear cycles. The first 500 abrasion cycles only made the CA decreased from 162.8° to 159°, and the CA of the sample was still higher than 155° after 800 cycles of abrasion. Further abrasion showed that the superhydrophobicity of the synthetic suede was very robust against 1600 abrasion cycles, with CA over 150°. After severe abrasion, the CA on the surface decreased to 150° with SA increased to about ±15°. The picture and SEM image of the Synthetic suede–PDMS–OTS after 2000 cycles of abrasion were displayed in Fig. 7(a) and (b). It was found that although the synthetic suede was abraded flat and got loss of some roughness of its surface, the sample is still not broken with repellency to water droplet. The durability of the superhydrophobicity of the suede might come from the combination of PDMS and OTS. PDMS as an elastomer has not only good wear resistance but also strong adhesive force to synthetic leather fibers after curing.[59] And OTS as additional low surface energy substance to PDMS, can be dehydrated and condensed to form a long-chain polymer, which can provide surface roughness and hydrophobization.[60] As the number of friction cycles increases, the surface condensed polymer from OTS is first worn away, and then the underlying PDMS. A composite coating formed by PDMS and OTS resulted in improvement of the superhydrophobicity and abrasion resistance of the suede surface. This demonstrated that the obtained Synthetic suede–PDMS–OTS has excellent mechanically resistant superhydrophobicity.

Chemical resistance of the superhydrophobic suede material was also evaluated. The Synthetic suede–PDMS–OTS was

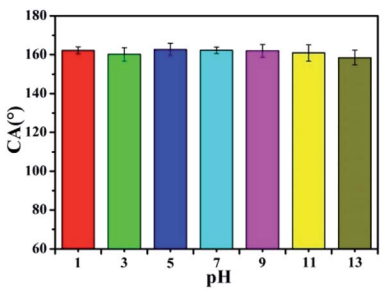

Fig. 8 CAs of the Synthetic suede–PDMS–OTS after immersion in different pH solutions for 3 days.

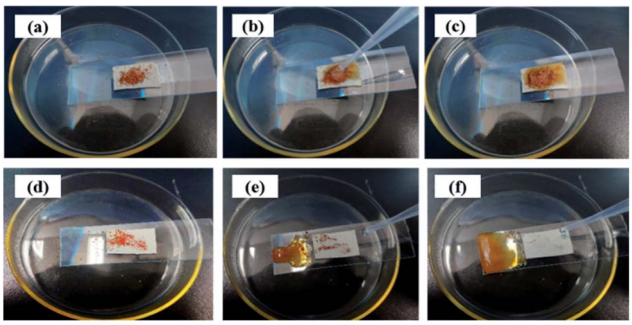

Fig. 9 Self-cleaning test of (a–c) pristine synthetic suede, and (d–f) Synthetic suede–PDMS–OTS.

immersed into different pH (pH = 1–13) solutions for 72 h, then rinsed by water and dried. As shown in Fig. 8, although a slight decrease of CA after immersion in a solution at pH 13 was observed, which might be caused by some hydrolysis of the ester groups formed by dehydration condensation of OTS under strong alkaline conditions, the CAs still remained above 150°. This might be because the air layer between the solution and the superhydrophobic surface prevented the synthetic suede from corrosion by acid or alkali solution, demonstrating that the Synthetic suede–PDMS–OTS is highly stable against chemical corrosion.

Self-cleaning performance was inspired by the phenomenon of lotus leaf in nature. Water droplets can keep the spherical shape and easily take the dust away due to the superhydrophobicity. Self-cleaning properties of the pristine and modified synthetic suede were tested here. Fine gravel dyed by methyl orange was used as a marker on the pristine synthetic suede and Synthetic suede–PDMS–OTS. It can be obviously seen from Fig. 9(a–c) that when rinsing with water droplets, the dye made the pristine synthetic suede totally wetted and polluted by the dyed fine gravels. However, the dyed fine gravel on the surface of Synthetic suede–PDMS–OTS was easily removed away by droplet without dyeing of the surface, as shown in Fig. 9(d–f). The result confirmed that the Synthetic suede–PDMS–OTS showed excellent self-cleaning property.

Conclusions

Using PDMS and OTS as low surface energy substances, superhydrophobic synthetic suede was prepared by step-by-step impregnation. The contact angle (CA) and sliding angle (SA) of the as-prepared synthetic suede were 162.8° and 3.4°, respectively. In addition, the as-fabricated synthetic suede can maintain its superhydrophobicity after 2000 times abrasion, showing a strong mechanical resistance. Importantly, the superhydrophobic synthetic suede has good self-cleaning and chemical resistant properties. This present fabrication method is facile and can be used for large area production of superhydrophobic synthetic suede materials.

Conflicts of interest

There are no conflicts to declare.

Acknowledgements

This work was supported by National Natural Science Foundation of China (51572161).

Notes and references

1 T. Ye, S. Bin and J. Lei, *Adv. Mater.*, 2015, **26**, 6872–6897.
2 Y. Liang, J. Shi, P. Xiao, J. He and T. Chen, *Chem. Commun.*, 2018, **54**, 12804–12807.
3 L. Zhao, L. Zhou, C. Sun, Y. Gu, W. Wen and X. Fang, *CrystEngComm*, 2018, **20**, 6529–6537.
4 C.-H. Xue, P. Zhang, J.-Z. Ma, P.-T. Ji, Y.-R. Li and S.-T. Jia, *Chem. Commun.*, 2013, **49**, 3588–3590.
5 J. Yong, F. Chen, Q. Yang, J. Huo and X. Hou, *Chem. Soc. Rev.*, 2017, **46**, 4168–4217.
6 W. K. Lee, W. B. Jung, S. R. Nagel and T. W. Odom, *Nano Lett.*, 2016, **16**, 3774–3779.
7 Z. Hu, X. Zhang, Z. Liu, K. Huo and J. Lei, *Adv. Funct. Mater.*, 2015, **24**, 6381–6388.
8 Y. Wu, J. Zeng, Y. Si, M. Chen and L. Wu, *ACS Nano*, 2018, **12**, 10338–10346.
9 Y. Zhu, F. Sun, H. Qian, H. Wang, L. Mu and J. Zhu, *Chem. Eng. J.*, 2018, **338**, 670–679.
10 Z. Guo and X. Jing, *J. Mater. Chem. A*, 2018, **6**, 16731–16768.
11 F. L. Heale, K. Page, J. S. Wixey, P. Taylor, I. P. Parkin and C. J. Carmalt, *RSC Adv.*, 2018, **8**, 27064–27072.
12 J. Huang, S. Li, M. Ge, L. Wang and Y. Lai, *J. Mater. Chem. A*, 2015, **3**, 2825–2832.
13 Y. Lu, S. Sathasivam, J. Song, C. R. Crick, C. J. Carmalt and I. P. Parkin, *Science*, 2018, **347**, 1132–1135.
14 C. Peng, Z. Chen and M. K. Tiwari, *Nat. Mater.*, 2018, **17**, 355–360.
15 Y. Si and Z. Guo, *Nanoscale*, 2015, **7**, 5922–5946.
16 S. Zhang, J. Huang, Y. Cheng, H. Yang, Z. Chen and Y. Lai, *Small*, 2017, **13**, 1701867.
17 C.-H. Xue and J.-Z. Ma, *J. Mater. Chem. A*, 2013, **1**, 4146–4161.
18 M. M. Bashar, H. Zhu, S. Yamamoto and M. Mitsuishi, *RSC Adv.*, 2017, **7**, 37168–37174.
19 L. Na, W. Xiaoli, P. Shitao, L. Lei and Z. Ran, *RSC Adv.*, 2018, **8**, 30257–30264.
20 J. Yong, J. Huo, F. Chen, Q. Yang and X. Hou, *Phys. Chem. Chem. Phys.*, 2018, **20**, 25140–25163.
21 S. Li, K. Page, S. Sathasivam, F. Heale, G. He, Y. Lu, Y. Lai, G. Chen, C. J. Carmalt and I. P. Parkin, *J. Mater. Chem. A*, 2018, **6**, 17633–17641.
22 L. Hui, J. Huang, C. Zhong, G. Chen, K. Q. Zhang, S. S. Aldeyab and Y. Lai, *Chem. Eng. J.*, 2017, **330**, 26–35.
23 Y. Zhang, J. Zhang and A. Wang, *J. Mater. Chem. A*, 2016, **4**, 901–907.
24 L. Wang, H. Wang, X. W. Huang, X. Song and J. Gao, *J. Mater. Chem. A*, 2018, **6**, 24523–24533.
25 S. Zheng, *Mater. Des.*, 2016, **93**, 261–270.
26 L. Wang, Q. Gong, S. Zhan, L. Jiang and Y. Zheng, *Adv. Mater.*, 2016, **28**, 7729–7735.
27 Z. Han, X. Feng, Z. Jiao, Z. Wang and L. Ren, *RSC Adv.*, 2018, **8**, 26497–26505.

28 K. Chen, S. Zhou and L. Wu, *ACS Nano*, 2016, **10**, 1386–1394.
29 C.-H. Xue, X.-J. Guo, J.-Z. Ma and S.-T. Jia, *ACS Appl. Mater. Interfaces*, 2015, **7**, 8251–8259.
30 U. G. M. Ekanayake, N. Rathuwadu and R. M. G. Rajapakse, *RSC Adv.*, 2018, **8**, 31406–31413.
31 R. Min, L. Wen, W. Baoshan, D. Binwei, M. Fumin and Y. Zhanlong, *Langmuir*, 2013, **29**, 8482–8491.
32 L. Zhang, C.-H. Xue, M. Cao, M.-M. Zhang, M. Li and J.-Z. Ma, *Chem. Eng. J.*, 2017, **320**, 244–252.
33 S. Wang, C. Liu, G. Liu, Z. Ming, L. Jian and C. Wang, *Appl. Surf. Sci.*, 2011, **258**, 806–810.
34 T. Urandelger, Y. Adem, O. Fahri Emre and B. Mehmet, *ACS Appl. Mater. Interfaces*, 2014, **6**, 9680–9688.
35 J. Gao, L. Wu, Z. Guo, J. Li, C. Xu and H. Xue, *J. Mater. Chem. C*, 2019, **7**, 4199–4209.
36 L. Li, Y. Bai, L. Li, S. Wang and T. Zhang, *Adv. Mater.*, 2017, **29**, 1702517.
37 M. Kerstin, W. Joshua Ray, V. R. Gabriela, M. J. Schoing and W. Joseph, *Analyst*, 2011, **136**, 2912–2917.
38 A. M. Rather and U. Manna, *J. Mater. Chem. A*, 2017, **5**, 15208–15216.
39 S. J. Ali, J. R. Rao and B. U. Nair, *Green Chem.*, 2000, **2**, 298–302.
40 J. Herndl and W. Haldemann, *J. Soc. Dyers Colour.*, 2013, **12**, 646–656.
41 P. S. Brown and B. Bhushan, *Philos. Trans. R. Soc., A*, 2016, **374**, 20160193.
42 X. Bai, C.-H. Xue and S.-T. Jia, *ACS Appl. Mater. Interfaces*, 2016, **8**, 28171–28179.
43 B. Li and J. Zhang, *Chem. Commun.*, 2016, **52**, 2744–2747.
44 T. Verho, C. Bower, P. Andrew, S. Franssila, O. Ikkala and R. H. Ras, *Adv. Mater.*, 2011, **23**, 673–678.
45 X. Deng, L. Mammen, Y. Zhao, P. Lellig, K. Mullen, C. Li, H. J. Butt and D. Vollmer, *Adv. Mater.*, 2011, **23**, 2962–2965.
46 G. Zhi and J. He, *J. Mater. Chem. A*, 2014, **2**, 16601–16607.
47 Z. Guo and X. Jing, *J. Mater. Chem. A*, 2018, **6**, 16731–16768.
48 M. M. Quazi, M. Ishak, A. Arslan, M. A. Fazal, F. Yusof, B. S. Sazzad, M. N. Bashir and M. Jamshaid, *RSC Adv.*, 2018, **8**, 6858–6869.
49 X. Kong, C. Zhu, J. Lv, J. Zhang and J. Feng, *Prog. Org. Coat.*, 2020, **138**, 105342.
50 C.-H. Xue, Z.-D. Zhang, J. Zhang and S.-T. Jia, *J. Mater. Chem. A*, 2014, **2**, 15001–15007.
51 X. Zhao, L. Ji, L. Qiao, Q. Liang, Z. Lei, L. Zhu and C. Yang, *RSC Adv.*, 2018, **8**, 25008–25013.
52 P. Wang, M. Chen, H. Han, X. Fan and Q. Liu, *J. Mater. Chem. A*, 2016, **4**, 7869–7874.
53 T. Sano and S. Suzuki, *Forensic Sci. Int.*, 2009, **192**, e27–e32.
54 J.-Z. Ma, X.-J. Lv, D.-G. Gao, Y. Li, B. Lv and J. Zhang, *J. Cleaner Prod.*, 2014, **72**, 120–126.
55 C.-H. Xue, P. Zhang, J.-Z. Ma, P.-T. Ji, Y.-R. Li and S.-T. Jia, *Chem. Commun.*, 2013, **49**, 3588–3590.
56 A. N. Parikh, M. A. Schivley, E. Koo, K. Seshadri, D. Aurentz, K. Mueller and D. L. Allara, *J. Am. Chem. Soc.*, 1997, **119**, 3135–3143.
57 M. Chen, D.-L. Zhou, Y. Chen and P.-X. Zhou, *J. Appl. Polym. Sci.*, 2006, **103**, 903–908.
58 E. J. Park, J. K. Sim, M.-G. Jeong, H. O. Seo and Y. D. Kim, *RSC Adv.*, 2013, **3**, 12571.
59 Q.-P. Ke, W.-Q. Fu, H.-L. Jin, T.-D. Tang and J.-F. Zhang, *Surf. Coat. Technol.*, 2011, **205**, 4910–4914.
60 H. Zhou, H.-X. Wang, H.-T. Niu, A. Gestos, X. G. Wang and T. Lin, *Adv. Mater.*, 2012, **24**, 2409–2412.